Kinetic and thermodynamic investigations of CO_2 gasification of coal chars prepared via conventional and microwave pyrolysis

Peng Jiang[1] · Yang Meng[1] · Ziyao Lu[1] · Lan Xu[1] · Gang Yang[2] · Xiang Luo[2] ·
Kaiqi Shi[2] · Tao Wu[1,2] ⓘ

Abstract This study examined an isothermal CO_2 gasification of four chars prepared via two different methods, i.e., conventional and microwave-assisted pyrolysis, by the approach of thermogravimetric analysis. Physical, chemical, and structural behaviours of chars were examined using ultimate analysis, X-ray diffraction, and scanning electronic microscopy. Kinetic parameters were calculated by applying the shrinking unreacted core (SCM) and random pore (RPM) models. Moreover, char-CO_2 gasification was further simulated by using Aspen Plus to investigate thermodynamic performances in terms of syngas composition and cold gas efficiency (CGE). The microwave-induced char has the largest C/H mass ratio and most ordered carbon structure, but the smallest gasification reactivity. Kinetic analysis indicates that the RPM is better for describing both gasification conversion and reaction rates of the studied chars, and the activation energies and pre-exponential factors varied in the range of 78.45–194.72 kJ/mol and 3.15–102,231.99 s^{-1}, respectively. In addition, a compensation effect was noted during gasification. Finally, the microwave-derived char exhibits better thermodynamic performances than the conventional chars, with the highest CGE and CO molar concentration of 1.30% and 86.18%, respectively. Increasing the pyrolysis temperature, gasification temperature, and CO_2-to-carbon molar ratio improved the CGE.

Keywords Coal char · CO_2 gasification · Microwave pyrolysis · Char properties · Kinetics · Thermodynamic

1 Introduction

Coal is a particularly important energy resource and is currently responsible for approximately 70% of total energy consumption in China (Lan et al. 2018; Zhu et al. 2020). Urgent development of clean coal utilization technology is required because of increasing environmental pollution from coal-fired power plants. Coal gasification, which converts solid coal into syngas at high temperatures, is considered to be the cleanest utilization approach because it offers near-zero sulphur and particulate emissions, high energy efficiency, and flexible chemicals (Attwood et al. 2003; Li et al. 2018). Char reaction with gasification agents is the rate-controlling step of the coal gasification process because it occurs more slowly than water evaporation, pyrolysis, or combustion (Dupont et al. 2011). As a greenhouse gas, CO_2 is the largest contributor to global warming (Fan et al. 2017). Hence, it is critical to implement CO_2 mitigation strategies that can help to alleviate climate change. Fortunately, the employment of CO_2 to gasify coal char for valuable syngas production emerges as a promising approach to reducing CO_2 accumulation. Therefore, studies on the kinetics and thermodynamic performances of char-CO_2 gasification are

✉ Tao Wu
tao.wu@nottingham.edu.cn

1 Department of Chemical and Environmental Engineering, The University of Nottingham Ningbo China, Ningbo 315100, China

2 Key Laboratory for Carbonaceous Wastes Processing and Process Intensification Research of Zhejiang Province, The University of Nottingham Ningbo China, Ningbo 315100, China

⧉ Springer

essential for the reactor design, control and efficiency (Zhang et al. 2010).

Char-CO_2 reactivity is greatly affected by char characteristics, which are determined mainly by coal pyrolysis conditions, of which the pyrolysis temperature is the most important parameter (Wang et al. 2016b). Microwave heating can produce rapid, volumetric, selective, non-contact heating of coal by directly converting electromagnetic energy into thermal energy (Parvez et al. 2019). This is quite different from conventional heating mechanisms in which heat is transferred from the coal surface to the coal interior via conduction (Wu et al. 2015). Previous investigations of microwave pyrolysis of coal were mainly focused on three areas: the effect of microwave pyrolysis on physicochemical properties such as coal grindability and dryness (Ge et al. 2013; Lester et al. 2005; Marland et al. 2000); dielectric properties, interaction mechanisms, and enhancement of coal pyrolysis using microwave absorbers (Liu et al. 2016; Monsef-Mirzai et al. 1995; Peng et al. 2012, 2017); and the properties of pyrolysis products such as gaseous material, tar, and char (Abdelsayed et al. 2018; Reddy et al. 2019; Reddy and Vinu 2016). Researchers also considered microwave reactors and their scale-up (Binner et al. 2014; Salema and Ani 2012). It was demonstrated that microwave pyrolysis showed more gaseous and less tar, high quality liquid fuels and more energy-efficient than conventional pyrolysis (Abdelsayed et al. 2018; Reddy and Vinu 2016).

However, studies on the structure, gasification reactivity, and kinetics of microwave-assisted coal char are rarely reported. Abdelsayed et al. (2018) investigated the effects of pyrolysis temperatures and microwave heating on product distributions and char structure changes of Mississippi coal char and tested the combustion reactivity using a non-isothermal thermogravimetric analysis (TGA). More recently, Liu et al. (2020) analysed the detailed evolutions of char structures and functional groups in low-temperature microwave-prepared char from Zhundong coal. The combustion reactivity of the microwave char was also performed. Results showed that microwave-induced char had a higher burnout temperature than that of conventional pyrolysis char. Nevertheless, little research has been performed on the gasification reactivity and kinetics of CO_2 iso-thermal gasification of coal chars prepared via microwave pyrolysis.

To ensure the implementation of CO_2 gasification, the prediction of thermodynamic performances for char-CO_2 gasification is of significant importance (Renganathan et al. 2012). Process simulations of biomass gasification using pure or mixer CO_2 have been carried out broadly (Cheng et al. 2016; Guizani et al. 2015; Renganathan et al. 2012; Sadhwani et al. 2017). As far as we acknowledged, no study has been conducted in detailed thermodynamic performances of coal char gasification with pure CO_2 as a gasifying medium.

In this study, char-CO_2 isothermal gasification kinetic behaviours and thermodynamic performances were investigated using thermogravimetric analysis and Aspen Plus, respectively. One char was derived via microwave pyrolysis, while the other three char samples were produced using conventional pyrolysis at different temperatures for the purpose of comparison. In addition, char chemical compositions, structures, and morphologies were analysed. Moreover, SCM and RPM methods were employed to calculate the kinetic parameters of all chars. Furthermore, thermodynamic performances including syngas composition and CGE of char-CO_2 gasification were assessed.

2 Materials and methods

2.1 Materials

Pulverised bituminous Qinghai coal was collected from a domestic power plant in China. The air-dried coal was ground and sieved. To avoid heat- and mass-transfer limitations during heating experiments, only particles smaller than 0.106 mm were collected. Conventional pyrolysis was performed in a horizontal tube furnace, where the coal pyrolysis temperatures were set at 1073, 1173 and 1273 K for 30 min under a pure N_2 atmosphere, respectively. The collected chars were stored separately in a dryer and labelled Py1073, Py1173, and Py1273, respectively. The microwave-derived char was prepared in a 2.45 GHz multi-mode microwave-cavity from Nanjing Jiequan Microwave Co., Ltd. Approximately 2.0 g of coal was blended with 20.0 g of silicon carbide (used as a microwave receptor to assist in coal pyrolysis) and pyrolyzed at 1173 K for 30 min. Detailed descriptions of microwave pyrolysis can be found in our previous work (Shi et al. 2017). Char derived from microwave pyrolysis was labelled MW.

Proximate and ultimate analyses of the coal and its derived chars were conducted using a thermos balance analyser (NETZSCH STA 449 PC Luxx, Germany) and a VarioE III Element Analyser (GmbH) according to GB/T 212–2008 and GB/T 476–2008, respectively. The results are presented in Table 1.

The morphology of char samples was examined using a SEM (Zeiss Sigma VP, Germany). Char crystal structures were measured using a powder XRD (Bruker D8 advanced A25) with Cu K$_\alpha$ radiation. The chars were scanned from 10° to 80°. The crystals were characterised quantitatively via their inter-layer spacings (d_{002}), stacking heights (L_c), and average number of crystallites in a stack (N_{mean}). Their expressions are illustrated as (Huo et al. 2014),

Table 1 Ultimate and proximate analysis of the samples

Sample	Proximate analysis (w_{ad} %)				Ultimate analysis (w_{ad} %)				
	A	V	M	FC	C	H	N	S	C/H
Coal	14.9	25.6	5.9	53.5	67.8	3.7	0.7	0.3	18.3
Py1073	16.7	5.3	3.5	74.6	75.2	1.7	0.8	0.9	29.1
Py1173	19.5	2.4	2.1	76	75.9	1.5	0.6	0.9	48.3
Py1273	19.8	0.6	2	77.6	76.5	1.3	0.6	0.9	62
MW	19.8	0.5	1.8	77.9	77.1	1.2	0.6	0.9	64.2

$$d_{002} = \frac{\lambda}{2\sin\theta_{002}} \tag{1}$$

$$L_c = \frac{0.89\lambda}{\beta_{002}\cos\theta_{002}} \tag{2}$$

$$N_{mean} = \frac{L_c}{d_{002}} + 1 \tag{3}$$

where λ is the wavelength of the X-ray and β is the peak width at half of the maximum intensity.

2.2 Gasification test

Isothermal gasification experiments were carried out using a thermogravimetric analyzer (NETZSCH STA 449 PC Luxx, Germany). The instrument was calibrated using the indium-aluminium check method prior to gasification testing. Each char sample (10 mg ± 0.5 mg) was heated to the gasification temperature at 25 K/min under a pure N₂ flow of 50 mL/min. When the gasification temperatures (1173, 1223, and 1273 K) were reached, the N₂ flow was replaced with a CO₂ flow (50 mL/min). Subsequently, the gasification temperature was kept constant for approximately 60 min under CO₂ atmosphere. The weight loss curve was recorded from room temperature to the end of gasification. Each experiment was replicated three times to ensure reproducibility. The experimental errors were within ± 2%. Gasification conversion (x) is calculated as (Dwivedi et al. 2019):

$$x = \frac{m_0 - m_t}{m_0 - m_{ash}} \tag{4}$$

where m_0 is the char mass at the start of gasification, m_t is the char mass at time t, and m_{ash} represents the mass of ash in the char.

The reactivity of different chars at various gasification temperatures were evaluated using the reactivity index, $R_{0.5}$, which is expressed as:

$$R_{0.5} = \frac{0.5}{t_{0.5}} \tag{5}$$

where $t_{0.5}$ represents the time required for char conversion of 50%. A higher reactivity indicates a better gasification performance.

2.3 Kinetic model

In general, the gasification rate for a heterogeneous reaction can be described as:

$$r = \frac{dx}{dt} = k(T)f(x) \tag{6}$$

$$k(T) = A\exp\left(-\frac{E_a}{RT}\right) \tag{7}$$

where A is the pre-exponential factor; E_a is the activation energy; and R is the universal gas constant, $R = 8.314$ J/(K mol). Here, $f(x)$ is the gasification mechanism function and x denotes carbon conversion.

In this study, the SCM and RPM were adopted as the mechanism functions to fit the experimental data due to their widely application in simulation of char gasification process (Wang et al. 2016a). The SCM considers that the gasification takes place at the char surface and moves inside. The SCM model is described as follows:

$$r = \frac{dx}{dt} = k_{SCM}(1-x)^{2/3} \tag{8}$$

The RPM assumes overlapping of pore surfaces. The gasification rate is shown as:

$$r = \frac{dx}{dt} = k_{RPM}(1-x)\sqrt{1-\psi\ln(1-x)} \tag{9}$$

where ψ is a structural parameter that is calculated using a regression method as follows:

$$\frac{t_x}{t_{0.8}} = \frac{\sqrt{1-\psi\ln(1-x)}-1}{\sqrt{1-\psi\ln(1-0.8)}-1} \tag{10}$$

The apparent rate constants of k_{SCM} and k_{RPM} can be obtained from the linear fit of the experimental data with the following expressions of SCM and RPM, respectively.

$$3\left[1-(1-x)^{1/3}\right] = k_{SCM}t \tag{11}$$

$$(2/\psi)\left[\sqrt{1-\psi\ln(1-x)}-1\right] = k_{RPM}t \tag{12}$$

After determination of the reaction rate constant, the activation energy and pre-exponential factor are determined by plotting $\ln k$ and $1/T$ via the following equation:

$$\ln k = -\frac{E_a}{RT} + \ln A \tag{13}$$

2.4 Aspen plus simulation

Considering the experimental char-CO_2 gasification temperature varied from 1173 to 1273 K, which are quite suitable for the operating temperature of a typical fluidized-bed gasifier. To evaluate the syngas composition and cold gas efficiency, thermodynamic modelling of char gasification using CO_2 was carried out using Aspen Plus (Li et al. 2014). Detailed simulation descriptions can be found in our previous work (Jiang et al. 2019, 2020). The CGE represents conversion of the char energy content to the lower heating value of syngas, as defined by Eqs. (14) and (15) (Renganathan et al. 2012).

$$CGE = \frac{LHV_{syg}}{LHV_{char}} \tag{14}$$

$$LHV_{syg} = n_{H_2}LHV_{H_2} + n_{CO}LHV_{CO} \tag{15}$$

where n and LHV refer to the molar flow rate and lower heating value, respectively. The subscripts H_2, CO, and char represent the corresponding species.

3 Results and discussion

3.1 Char characterization

As shown in Table 1, both the volatile and moisture contents of the conventional chars decrease as the pyrolysis temperature increases. In contrast, fixed carbon is observed to have a ppositive relation with the pyrolysis temperature. As the temperature varies from 1073 to 1273 K, the carbon content and C/H mass ratio increase from 75.2% to 76.5% and from 29.1 to 62.0, respectively. This is expected since high temperatures favour hydrocarbon cracking, which leads to more complete devolatilization. The MW char exhibits the lowest volatile, moisture, and hydrogen contents, but the highest fixed carbon content and C/H ratio. This is mainly determined by the nature of microwaves, which directly convert electromagnetic energy into thermal energy at the centre of the char, thus producing a faster heating rate than conventional heating (Wu et al. 2015). Consequently, more volatile components inside the char are released at high temperatures and higher fixed carbon contents and C/H ratios are obtained.

The crystallinities and structural parameters of the raw coal and pyrolyzed chars were investigated via XRD. The results are displayed in Fig. 1 and Table 2, respectively. Several sharp crystalline diffraction peaks were observed, such as those at 20.8° and 26.6°, which represent the inorganic mineral SiO_2. In addition, a broad diffraction peak is noted at the 2θ angle from 20° to 30°. It corresponds to the (002) carbon crystallite band. Chars prepared at different pyrolysis temperatures exhibit similar diffraction peaks, but the intensity of the (002) diffraction peak increases slightly with the pyrolysis temperature. These phenomena suggest that the microcrystalline structure is prone to becoming ordered. The structural parameters d_{002}, L_c, and N_{mean} are employed to quantify the crystal characteristics of all samples as displayed in Table 2. MW char exhibits the smallest d_{002} of 3.47 Å, which is similar to that of the well-ordered graphite (3.354 Å). Increasing the pyrolysis temperature reduces the d_{002} of conventional chars from 3.72 Å to 3.65 Å. The L_c and N_{mean} increase
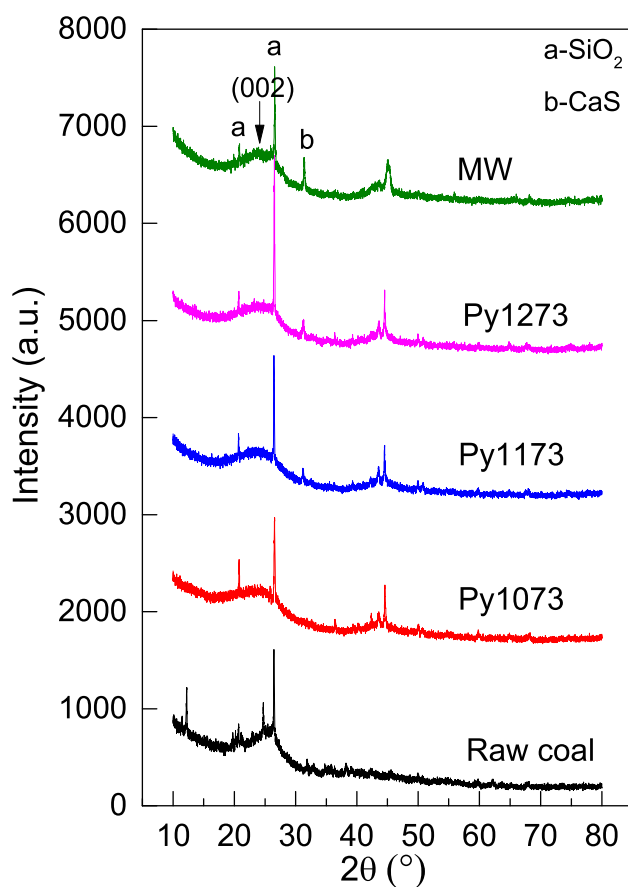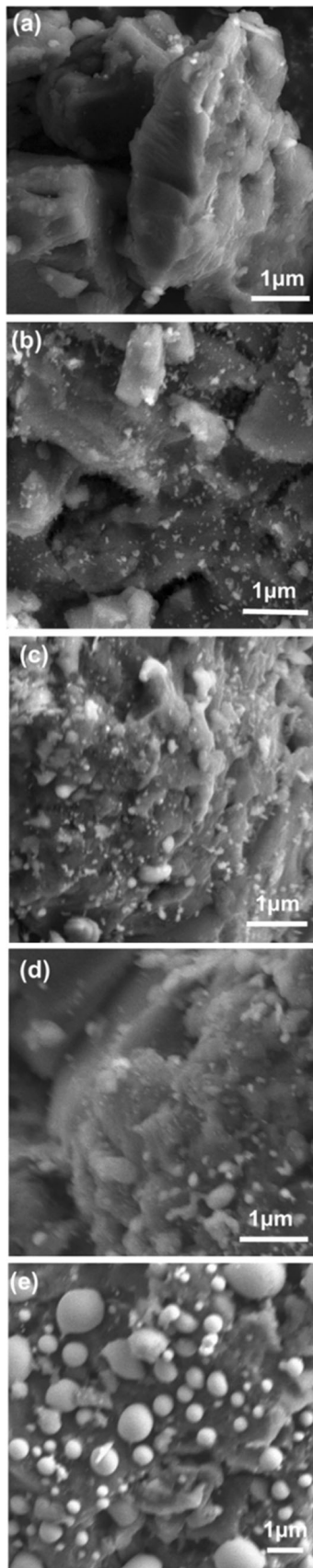

Fig. 1 XRD patterns from raw coal and pyrolyzed chars after conventional and microwave processing

Table 2 Structural parameters of coal and chars

Sample	d_{002} (Å)	L_c (Å)	N_{mean}
Py1073	3.72	13.80	4.71
Py1173	3.69	15.60	5.22
Py1273	3.65	17.43	5.77
MW	3.47	20.30	6.83

◄**Fig. 2** SEM images of five samples: **a** raw coal; **b** Py1073 char; **c** Py1173 char; **d** Py1273 char; and **e** MW char

from 13.8 Å to 17.43 Å and from 4.71 to 5.77, respectively, with the pyrolysis temperature from 1073 to 1273 K. In addition, the MW char exhibits the highest L_c and N_{mean}, suggesting greater crystallinity. Increasing the pyrolysis temperature can enhance cross-linking via dehydration and decarboxylation and even the dehydrogenation and aromatization reactions, resulting in the increasing ordered structures and also creating new ordered carbons (Abdelsayed et al. 2018). The microwave-induced char has the most ordered structure due to hot-spot formation under microwave heating. Such hot-spots can result in temperatures that are far higher than those in bulk char (Liu et al. 2019). As a consequence, MW char is more ordered and more thermally stable.

The morphological characteristics of the raw coal and its derived four chars are revealed by the SEM images presented in Fig. 2. The raw coal clearly exhibits a non-porous, blocky shape with a rough surface. The char samples produced via conventional pyrolysis are similar, but more pores and cavities are detected as the pyrolysis temperature increases, as shown in Figs. 2b–d. Besides, the surfaces are prone to be smooth and some microspheres appear as the pyrolysis temperature increases. Due to the release of volatile, some surface pores are formed on the surfaces and the addition of pyrolysis temperature leads particles to fuse and minerals to melt, resulting in the formation of smooth surfaces and microspheres.

In terms of MW char in Fig. 2e, its surface presents a more open structure due to the crack of internal small pores caused by rapid heating expansion. Besides, different size of microspheres with diameter varying from 0.2 to 1 μm are exhibited. This is driven primarily by high localised temperatures in the hot-spots formed via microwave heating (Abdelsayed et al. 2018). As a consequence, minerals are melted to form such microspheres.

Table 3 Summary of reactivity index ($R_{0.5}$) values

Sample	$R_{0.5}$ (10^3/s)		
	1173 K	1223 K	1273 K
Py1073	1.35	1.74	2.37
Py1173	1.07	1.51	2.26
Py1273	0.68	1.48	1.95
MW	0.39	1.08	1.92

3.2 Kinetic parameters

The reactivity of chars is quantified using the reactivity index, $R_{0.5}$, as detailed in Table 3. As the pyrolysis temperature increases from 1073 to 1273 K at a gasification temperature of 1173 K, $R_{0.5}$ decreases from 1.35 to 0.68.
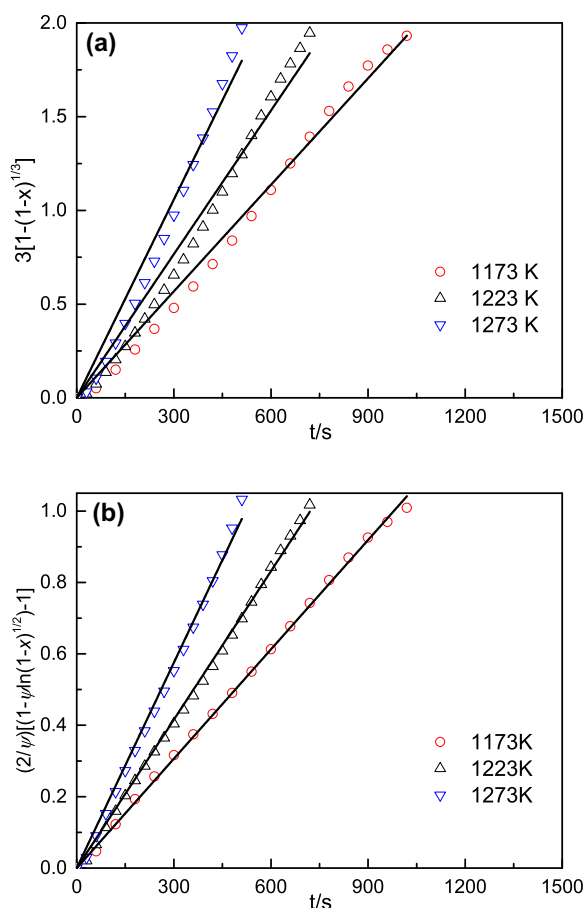

Fig. 3 Rate constant determination for the Py1073 char sample: a k_{SCM} and b k_{RPM}

This indicates that the Py1073 char has better gasification reactivity. Similar results can be found at different gasification temperatures. Meanwhile, $R_{0.5}$ has a positive relationship with the gasification temperature. As the conventional char pyrolysis temperature increases from 1173 to 1273 K, the reactivity index increases by 0.75–1.86 times. This suggests that higher gasification temperatures help char gasification. Microwave induced char has a smaller $R_{0.5}$ than conventional chars formed at the same gasification temperature. Increasing the char preparation temperature not only decreases the quantity of volatile matter, but also increases the extent of cross-linking. As a result, the C/H ratio decreases and the carbon structure becomes more ordered, as seen in Table 1 and Fig. 1, respectively. Hence, the reactivity of char gasification is ranked: Py1073 > Py1173 > Py1273 > MW.

The determination of kinetic parameters include reaction constant, pre-exponential factor and activation energy. By plotting $3[1 - (1 - x)^{1/3}]$ and $(2/\psi)\left[\sqrt{1 - \psi \ln(1 - x)} - 1\right]$ versus time (t), the reaction constants of k_{SCM} and k_{RPM} are obtained as the slopes of linearised curves at various gasification temperatures. Figure 3 presents a calculating example for the determination of k_{SCM} and k_{RPM} for the Py1073 char. It is worth noting that the value of structural constant φ is determined by plotting of ($t_x/t_{0.8}$) as a function of conversion as shown in Eq. (10) for chars exposed to various gasification temperatures. The φ values are regressed to be 8.2, 7.5, 2.8, and 2 for Py1073, Py1173, Py1273, and MW, respectively. This indicates that MW undergoes less pore development during gasification. This result is in accordance with the finding by Liu et al. (2020) that conventional pyrolysis is more conducive to pore development than microwave treatment. Table 4 summarises the rate constants for the two kinetic models. The coefficients of determination (R^2) are also listed to show the effectiveness of fitting. As shown, the R^2 exceeds 0.99 in all cases suggesting

Table 4 k values obtained via linear fits of the experimental data and the coefficients of determination

Char sample	Model	Reaction rate constant k (10^{-4}/s)					
		1173 K	R^2	1223 K	R^2	1273 K	R^2
Py1073	SCM	18.9	0.9984	25.5	0.9967	35.3	0.9952
	RPM	10.2	0.9998	13.9	0.9997	19.2	0.9984
Py1173	SCM	15.1	0.9975	22.1	0.9941	35.9	0.9883
	RPM	8.4	0.9996	12.3	0.9995	19.8	0.9976
Py1273	SCM	8.2	0.9985	19.1	0.9992	27.6	0.9946
	RPM	6.73	0.9991	15.1	0.9994	20.6	0.9974
MW	SCM	2.40	0.9987	6.14	0.9985	11.7	0.9982
	RPM	2.11	0.9988	5.26	0.9985	10.1	0.9985

excellent correlation. The resulting values of k_{SCM} and k_{RPM} are different for the same char under the same gasification temperature. As the gasification temperature increases, both k_{SCM} and k_{RPM} increase by about 1.86–4.88 times. Nevertheless, given a particular gasification temperature, both k_{SCM} and k_{RPM} decrease with the pyrolysis

Fig. 4 Determination of the kinetic parameters (A and E_a) from the SCM and RPM models: **a** Py1073 char; **b** Py1173 char; **c** Py1273 char; and **d** MW char

temperature, indicating the reduction of reactivity. Based on the calculated k values, the activation energy and pre-exponential factor are determined using the Arrhenius equation shown in Eq. (13). Figure 4 shows plots of ln$k$ versus $1/T$ using various models. Clearly, there is a good linear fit between ln$k$ and 1/T.

Table 5 summarises the kinetic parameters calculated using the slopes and intercepts in Fig. 4. There are slight differences between the E_a and A values obtained via the SCM and RPM methods. In addition, the pyrolysis temperature and use of microwave heating for char preparation have significant effects on the E_a and A, which vary from 78.45 to 194.72 kJ/mol and from 3.15 to 102, 231.99 s⁻¹, respectively, using the RPM approach. It is also noticeable that there exists a "compensation effect" as the increase of A when E_a increases (Xu et al. 2019).

To find the best imitative gasification reaction model, the carbon conversion is calculated for all chars as a function of the gasification time at various gasification temperatures. Figure 5 compares the conversions predicted using the SCM and RPM methods to the experimental values. Visually, both models fit the conversion well. However, the RPM prediction is better than the SCM prediction, as the latter exhibits a relatively large discrepancy at times shorter than 800 s, as shown clearly in Fig. 5a, b. To quantify the effectiveness of fitting, both the R^2 and root mean square error (RMSE) are calculated for all chars and are displayed in Table 6. The R^2 of SCM conversion prediction varies from 0.955 to 0.994, while R^2 for RPM prediction ranges from 0.992 to 0.999. In addition, the RMSE values for RPM are between 0.0084 and 0.0251, but the RMSE varies from 0.016 to 0.067 for the SCM. This means that the RPM is the most suitable model for describing gasification conversion.

Variation of r in terms of x is also calculated using both the SCM and the RPM. The predictions are compared to experimental data in Fig. 6. The reaction rate increases until it reaches its maximum at approximately 0.15–0.40. This is followed by a decrease as conversion continues. The reaction rate decrease is attributed primarily to overlapping of inner pores, which leads to reduction of the
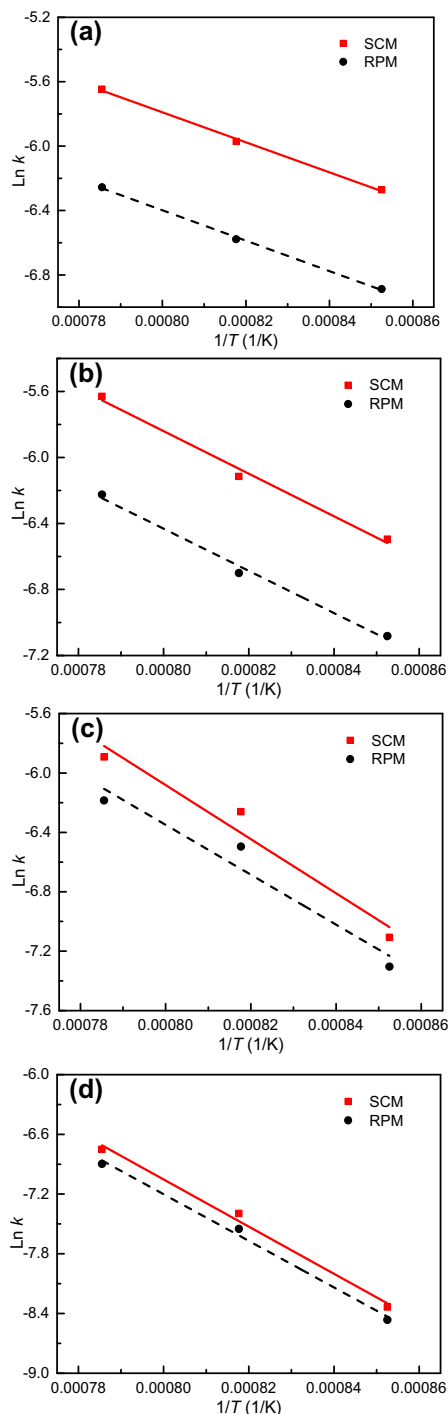
Table 5 Intrinsic SCM and RPM model kinetic parameters of materials made using various pyrolysis temperatures

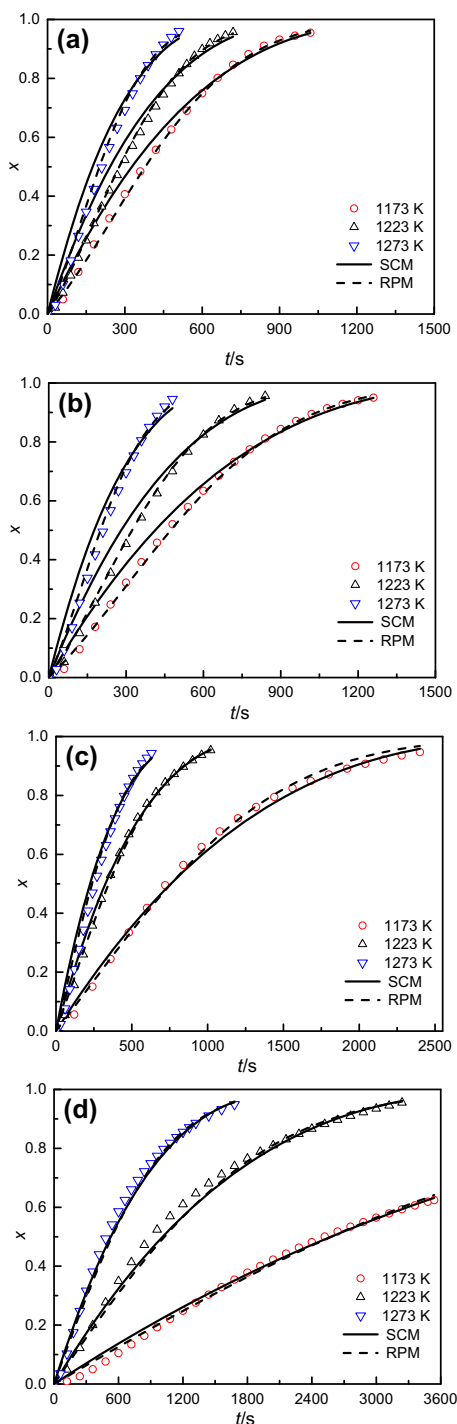| Char sample	SCM		RPM	
	A (s⁻¹)	E_a (kJ/mol)	A (s⁻¹)	E_a (kJ/mol)
Py1073	5.25	77.47	3.15	78.45
Py1173	88.49	107.28	44.25	106.23
Py1273	4817.45	151.39	1187.97	139.65
MW	148,301.11	197.05	102,231.99	194.72

Fig. 5 Comparison of RPM-and SCM-predicted conversions to experimental values: **a** Py1073 char; **b** Py1173 char; **c** Py1273 char; and **d** MW char

reaction surface area and active points (Wang et al. 2016a; Xu et al. 2019). The RPM fits the reaction rate data better than the SCM. Table 6 also shows the R^2 and RMSE values used to quantify reaction rate prediction effectiveness. For a given case, the RPM offers a higher R^2 and lower RMSE than its counterpart. Hence, the RPM approach is the best for capturing the reaction rate.

3.3 Thermodynamic analysis

As previously noted, the influences of the pyrolysis temperature and pyrolysis approach have significant impacts on the char structure and kinetic parameters. To exhibit the char-CO_2 gasification performances including syngas composition and cold gas efficiency under typical fluidized gasifiers using the above four derived chars as the raw materials, Aspen Plus simulation are carried out under the gasification at 1273 K and a CO_2-to-carbon molar ratio (CO_2/C, which is defined as the molar ratio between CO_2 fed to gasifier and carbon content in the char) of 1. The simulation result is depicted in Fig. 7a. The molar concentration of CO exceeds 82% and the molar concentrations of CO_2 and H_2 are approximately 8% and 4%, respectively, in the syngas. When the pyrolysis temperature increases from 1073 to 1273 K, the CO fraction gradually increases from 82.09% to 85.58%, while both the CO_2 and H_2 fractions decrease moderately. The microwave-induced char produces the highest CO concentration of 86.18% and smallest quantities of CO_2 and H_2. This is primarily because the MW sample has the largest C/H ratio, followed by Py1273, Py1173, and Py1073. Given fixed gasification conditions, the higher carbon content in the char generates more CO specie and thus produces a larger CO fraction. The CGE has the similar change tendency as the CO concentration, changing slightly from 1.27 to 1.30. The reason is mainly due to the addition of CO concentration and the LHV of CO is larger than that of H_2. Consequently, an increased CGE is expected according to Eqs. (14) and (15). It is clear that the CGE value exceeds 1 because syngas has a larger LHV than the original char caused by the conversion of CO_2 to CO.

Figure 7b presents the influence of the gasification temperature on gasification performances for the char Py1073 at CO_2/C = 1. Both the CO molar fraction and CGE increase slightly from 88.69% to 88.78% and from 1.266 to 1.267, respectively, when the gasification

Table 6 Comparison of evaluation indexes based on the SCM and RPM models

| Char type | Variable | SCM at 1173 K | | SCM at 1223 K | | SCM at 1273 K | | RPM at 1173 K | | RPM at 1223 K | | RPM at 1273 K | |
		R^2	RMSE	R^2	RMSE	R^2	RMSE	R^2	RMSE	R^2	RMSE	R^2	RMSE
Py1073	x	0.981	0.0400	0.963	0.03960	0.955	0.0620	0.999	0.00840	0.998	0.00890	0.997	0.0230
	r	0.831	0.0002	0.832	0.00009	0.776	0.0003	0.967	0.00008	0.969	0.00007	0.942	0.0001
Py1173	x	0.981	0.0520	0.993	0.05400	0.948	0.0670	0.999	0.01220	0.998	0.01200	0.992	0.0250
	r	0.946	0.0002	0.647	0.00027	0.618	0.0004	0.970	0.00009	0.985	0.00006	0.961	0.0002
Py1273	x	0.994	0.0615	0.992	0.06700	0.971	0.0490	0.996	0.02260	0.997	0.02400	0.991	0.0260
	r	0.928	0.00053	0.905	0.00040	0.859	0.0030	0.955	0.00017	0.963	0.00016	0.943	0.0020
MW	x	0.992	0.0160	0.992	0.02200	0.994	0.0210	0.996	0.01350	0.992	0.02510	0.995	0.0210
	r	0.731	0.00004	0.920	0.00005	0.922	0.0002	0.751	0.00003	0.921	0.00005	0.932	0.0001

temperature increases from 1173 to 1273 K. In terms of H_2 concentration, it exhibits a moderate decreasing trend from 7.21% to 7.12%. The increased gasification temperature helps the endothermic Boudouard reaction ($C + CO_2 \rightarrow CO$), which leads to enhancement of char-CO_2 gasification. Besides, the addition of temperature inhibits the exothermic water gas shift reaction ($CO + H_2O \rightarrow H_2 + CO_2$). Hence, the CO concentration increases and the H_2 concentration is reduced. Since CO production is favoured, the CGE increases with the gasification temperature.

The CO_2/C ratio is an important parameter because it directly determines the char conversion ratio and syngas composition. Figure 7c shows the effect of changing the CO_2/C ratio from 0.5 to 1.2 at a gasification temperature of 1273 K when testing the char of Py1073. Upon increasing CO_2/C, the CO concentration initially increases and then decreases moderately. Its maximum fraction is 93.8% at $CO_2/C = 0.94$. Nevertheless, increasing CO_2/C from 0.5 to 1.2 reduces the H_2 concentration from 13.0% to 5.7%. The CGE first increases from 0.74 to 1.22 and then is constant at 1.26 when $CO_2/C = 0.94$. When $CO_2/C < 0.94$, the carbon in the char is not fully gasified. The increased CO_2 flow rate contributes to increasing the CO concentration via the Boudouard reaction. Meanwhile, the H_2 concentration decreases because of the reverse WGS reaction. When $CO_2/C > 0.94$, the molar flowrate of CO remains unchanged. However, continued addition of CO_2 lowers both the CO and H_2 mol fractions after all of the carbon in the char is gasified with CO_2. As a consequence, the CGE first increases and then levels off.

4 Conclusions

This study investigated the char structure, morphological evolution, kinetics, and thermodynamics of coal char-CO_2 gasification using XRD, SEM, TGA, and Aspen Plus. Three chars were prepared using conventional heating conditions at 1073, 1173 and 1273 K, while one char was derived via microwave pyrolysis at 1173 K. The main conclusions are as follows.

(1) Increasing the pyrolysis temperature enhanced the C/H mass ratio and crystallinity in the char. The microwave-induced char had the highest C/H ratio and most ordered carbon structure. Clear microspheres were observed in the MW char due to hot-spot formation.

(2) During gasification, the MW char was less reactive than conventional chars.

(3) The kinetic parameters were determined using the SCM and RPM methods. Comparison of R^2 values indicated that the RPM was better at fitting the gasification conversion and reaction rate experimental data than the SCM. The activation energy and pre-exponential factor were in the range of 78.45–194.72 kJ/mol and 3.15–102,231.99 s^{-1}, respectively. A compensation effect was also noted during the gasification process.

(4) The MW char had the best thermodynamic performance, with the highest cold gas efficiency of 1.3 and CO molar concentration of 86.18%. Increasing
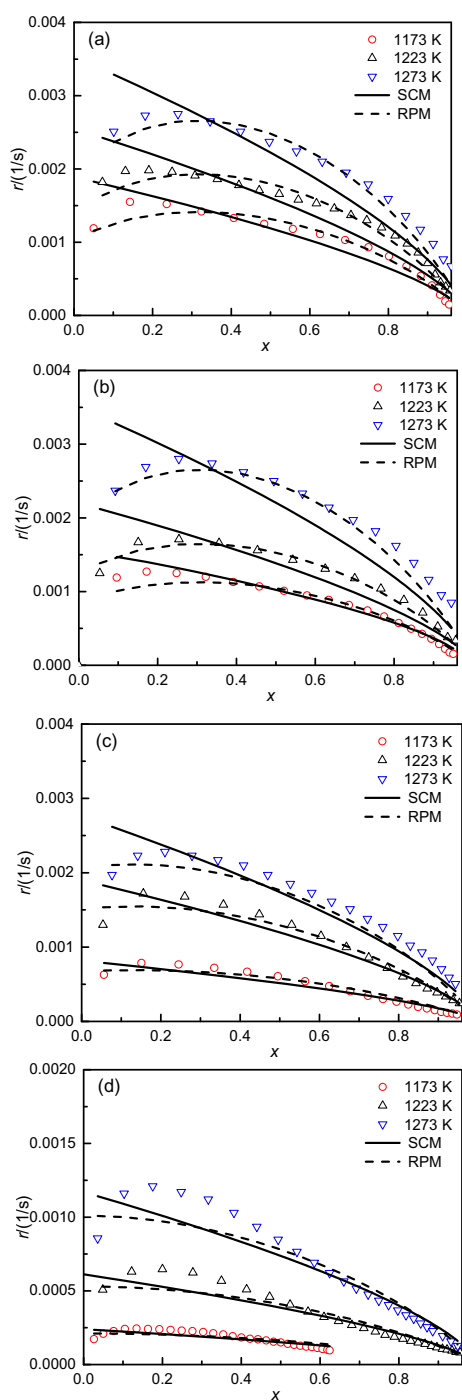
Fig. 6 Comparison of SCM- and RPM-predicted reaction rates to experimental values: **a** Py1073; **b** Py1173; **c** Py1273; and **d** MW char

the pyrolysis temperature, gasification temperature, and CO₂-to-carbon molar ratio could enhance the cold gas efficiency.
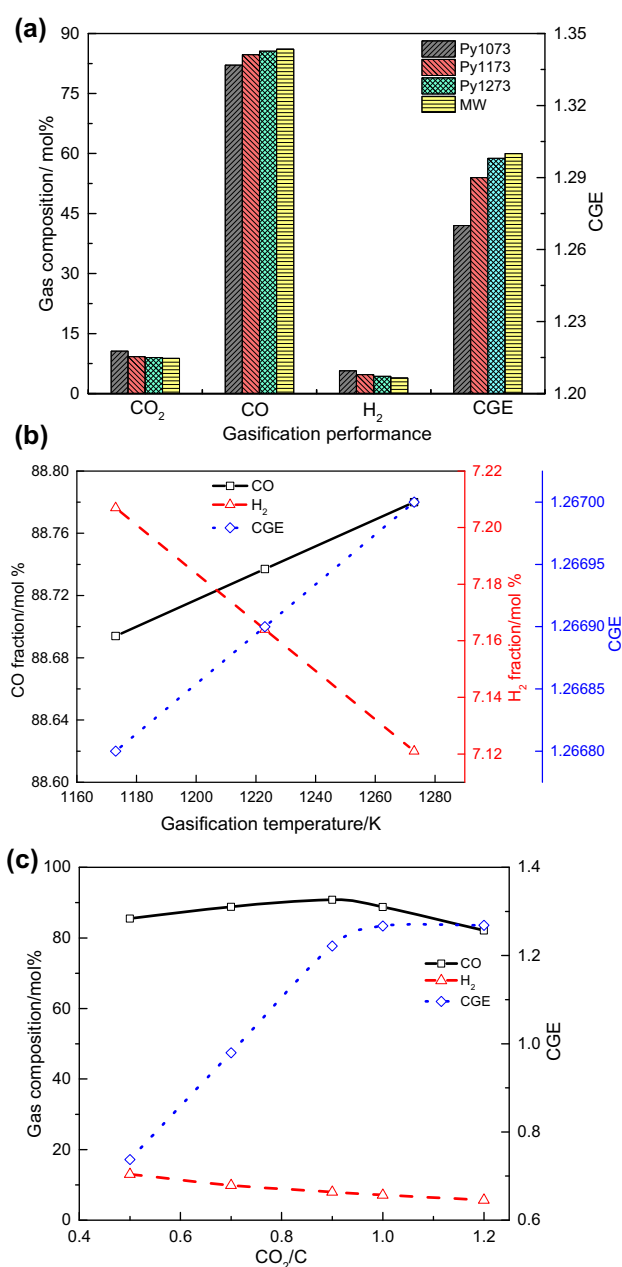

Fig. 7 Gasification performance of the char-CO_2 system: Effects of **a** the pyrolysis temperature, **b** the gasification temperature, and **c** the CO_2/C molar ratio

Conflict of interest The authors declare no conflicts of interest.

References

Abdelsayed V, Shekhawat D, Smith MW et al (2018) Microwave-assisted pyrolysis of Mississippi coal: a comparative study with conventional pyrolysis. Fuel 217:656–667

Attwood T, Fung V, Clark WW (2003) Market opportunities for coal gasification in China. J Clean Prod 11:473–479

Binner E, Lester E, Kingman S et al (2014) A review of microwave coal processing. J Microw Power Electromagn Energy 48:35–60

Cheng Y, Thow Z, Wang C-H (2016) Biomass gasification with CO₂ in a fluidized bed. Powder Technol 296:87–101

Dupont C, Nocquet T, Da Costa Jr JA et al (2011) Kinetic modelling of steam gasification of various woody biomass chars: influence of inorganic elements. Bioresour Technol 102:9743–9748

Dwivedi KK, Chatterjee P, Karmakar M et al (2019) Pyrolysis characteristics and kinetics of Indian low rank coal using thermogravimetric analysis. Int J Coal Sci Technol 6:102–112

Fan J, Hong H, Zhu L et al (2017) Thermodynamic evaluation of chemical looping combustion for combined cooling heating and power production driven by coal. Energy Convers Manag 135:200–211

Ge L, Zhang Y, Wang Z et al (2013) Effects of microwave irradiation treatment on physicochemical characteristics of Chinese low-rank coals. Energy Convers Manag 71:84–91

Guizani C, Louisnard O, Sanz FJE et al (2015) Gasification of woody biomass under high heating rate conditions in pure CO₂: experiments and modelling. Biomass Bioenergy 83:169–182

Huo W, Zhou Z, Chen X et al (2014) Study on CO₂ gasification reactivity and physical characteristics of biomass, petroleum coke and coal chars. Bioresour Technol 159:143–149

Jiang P, Parvez AM, Meng Y et al (2019) Exergetic, economic and carbon emission studies of bio-olefin production via indirect steam gasification process. Energy 187:115933

Jiang P, Guo D, Luo X et al (2020) Comparative study of the gasification of coal and its macerals and prediction of the synergistic effects under typical entrained-bed pulverized coal gasification conditions. J Energy Resour Technol 142:032203

Lan C, Lyu Q, Qie Y et al (2018) Thermodynamic and kinetic behaviors of coal gasification. Thermochim Acta 666:174–180

Lester E, Kingman S, Dodds C (2005) Increased coal grindability as a result of microwave pretreatment at economic energy inputs. Fuel 84:423–427

Li H, Yu Y, Han M et al (2014) Simulation of coal char gasification using O₂/CO₂. Int J Coal Sci Technol 1:81–87

Li C, Bai H, Lu Y et al (2018) Life-cycle assessment for coal-based methanol production in China. J Clean Prod 188:1004–1017

Liu H-P, Chen T-P, Li Y et al (2016) Temperature rise characteristics of ZhunDong coal during microwave pyrolysis. Fuel Process Technol 148:317–323

Liu Q, He H, Li H et al (2019) Characteristics and kinetics of coal char steam gasification under microwave heating. Fuel 256:115899

Liu H, Chen T, Fang L (2020) Evolution of char structure during non-isothermal low temperature pyrolysis of ZhunDong coal by microwave heating: a comparative study with conventional heating. J Energy Inst 93:1195–1206

Marland S, Han B, Merchant A et al (2000) The effect of microwave radiation on coal grindability. Fuel 79:1283–1288

Monsef-Mirzai P, Ravindran M, McWhinnie WR et al (1995) Rapid microwave pyrolysis of coal: methodology and examination of the residual and volatile phases. Fuel 74:20–27

Parvez AM, Wu T, Hong Y et al (2019) Gasification reactivity and synergistic effect of conventional and microwave pyrolysis derived algae chars in CO₂ atmosphere. J Energy Inst 92:730–740

Peng Z, Hwang J-Y, Kim B-G et al (2012) Microwave absorption capability of high volatile bituminous coal during pyrolysis. Energy Fuels 26:5146–5151

Peng Z, Lin X, Li Z et al (2017) Dielectric characterization of Indonesian low-rank coal for microwave processing. Fuel Process Technol 156:171–177

Reddy BR, Vinu R (2016) Microwave assisted pyrolysis of Indian and Indonesian coals and product characterization. Fuel Process Technol 154:96–103

Reddy BR, Shravani B, Das B et al (2019) Microwave-assisted and analytical pyrolysis of coking and non-coking coals: comparison of tar and char compositions. J Anal Appl Pyrol 142:104614

Renganathan T, Yadav M, Pushpavanam S et al (2012) CO₂ utilization for gasification of carbonaceous feedstocks: a thermodynamic analysis. Chem Eng Sci 83:159–170

Sadhwani N, Li P, Eden MR et al (2017) Process modeling of fluidized bed biomass-CO₂ gasification using ASPEN Plus. In: Espuña A, Graells M, Puigjaner L (eds). Computer aided chemical engineering, vol 40. pp: 2509–2514

Salema AA, Ani FN (2012) Pyrolysis of oil palm empty fruit bunch biomass pellets using multimode microwave irradiation. Bioresour Technol 125:102–107

Shi K, Yan J, Luo X et al (2017) Microwave-assisted pyrolysis of bamboo coupled with reforming by activated carbon for the production of hydrogen-rich syngas. Energy Procedia 142:1640–1646

Wang G, Zhang J, Shao J et al (2016a) Experimental and modeling studies on CO₂ gasification of biomass chars. Energy 114:143–154

Wang Q, Zhang R, Luo Z et al (2016b) Effects of pyrolysis atmosphere and temperature on coal char characteristics and gasification reactivity. Energy Technol 4:543–550

Wu C, Budarin VL, Wang M et al (2015) CO₂ gasification of bio-char derived from conventional and microwave pyrolysis. Appl Energ 157:533–539

Xu J, Zuo H, Wang G et al (2019) Gasification mechanism and kinetics analysis of coke using distributed activation energy model (DAEM). Appl Therm Eng 152:605–614

Zhang Y, Hara S, Kajitani S et al (2010) Modeling of catalytic gasification kinetics of coal char and carbon. Fuel 89:152–157

Zhu T, Wang R, Yi N et al (2020) CO₂ and SO₂ emission characteristics of the whole process industry chain of coal processing and utilization in China. Int J Coal Sci Technol 7:1–7